

LOW-RANK TENSOR PRODUCT RICHARDSON ITERATION FOR RADIATIVE TRANSFER IN PLANE-PARALLEL GEOMETRY

MARKUS BACHMAYR ^{*}, RICCARDO BARDIN [†], AND MATTHIAS SCHLOTTBOM [‡]

Abstract. The radiative transfer equation (RTE) has been established as a fundamental tool for the description of energy transport, absorption and scattering in many relevant societal applications, and requires numerical approximations. However, classical numerical algorithms scale unfavorably with respect to the dimensionality of such radiative transfer problems, where solutions depend on physical as well as angular variables. In this paper we address this dimensionality issue by developing a low-rank tensor product framework for the RTE in plane-parallel geometry. We exploit the tensor product nature of the phase space to recover an operator equation where the operator is given by a short sum of Kronecker products. This equation is solved by a preconditioned and rank-controlled Richardson iteration in Hilbert spaces. Using exponential sums approximations we construct a preconditioner that is compatible with the low-rank tensor product framework. The use of suitable preconditioning techniques yields a transformation of the operator equation in Hilbert space into a sequence space with Euclidean inner product, enabling rigorous error and rank control in the Euclidean metric.

Key words. isotropic radiative transfer, low-rank methods, iterative methods, compression, rank-control techniques, tensor product structure

AMS subject classifications. 65F10, 65F55, 65N22, 65N30

1. Introduction. Radiative transfer, that is, the phenomenon of energy transfer in the form of electromagnetic radiation including absorption and scattering, has many practical applications. Examples are medical imaging and tumor treatment [2, 4, 25], energy efficient generation of white light [29], climate sciences [18, 31], and geosciences [26]. In its stationary form, the interactions between the radiation and the medium are modeled by the radiative transfer equation (RTE),

$$(1.1) \quad \mathbf{s} \cdot \nabla \varphi(\mathbf{r}, \mathbf{s}) + \sigma_t(\mathbf{r})\varphi(\mathbf{r}, \mathbf{s}) = \sigma_s(\mathbf{r}) \int_S k(\mathbf{s} \cdot \mathbf{s}')\varphi(\mathbf{r}, \mathbf{s}') ds' + q(\mathbf{r}, \mathbf{s}) \quad \text{on } D \times S$$

where the specific intensity $\varphi = \varphi(\mathbf{r}, \mathbf{s})$ depends on the spatial coordinate $\mathbf{r} \in D \subset \mathbb{R}^d$ and on the direction $\mathbf{s} \in S$, with S denoting the unit sphere in \mathbb{R}^d . The gradient appearing in (1.1) is taken with respect to \mathbf{r} only. The physical properties of the medium covered by D enter (1.1) through the total attenuation (or transport) coefficient $\sigma_t(\mathbf{r}) = \sigma_a(\mathbf{r}) + \sigma_s(\mathbf{r})$, which accounts for the absorption and scattering rates, respectively, and through the scattering kernel $k(\mathbf{s} \cdot \mathbf{s}')$, which describes the probability of scattering from direction \mathbf{s}' into direction \mathbf{s} . Internal sources of radiation are modeled by the function $q(\mathbf{r}, \mathbf{s})$. We complement (1.1) by homogeneous inflow boundary conditions

$$(1.2) \quad \varphi(\mathbf{r}, \mathbf{s}) = 0 \quad \text{for } (\mathbf{r}, \mathbf{s}) \in \partial D_- := \{(\mathbf{r}, \mathbf{s}) \in \partial D \times S : \mathbf{n}(\mathbf{r}) \cdot \mathbf{s} < 0\}.$$

Here $\mathbf{n}(\mathbf{r})$ denotes the outward normal unit vector field for a point $\mathbf{r} \in \partial D$. We refer to [10, 11, 15] for further details on the derivation of the radiative transfer equation.

^{*}Institut für Geometrie und Praktische Mathematik, RWTH Aachen University, Templergraben 55, 52056 Aachen, Germany. bachmayr@igpm.rwth-aachen.de

[†]Department of Applied Mathematics, University of Twente, P.O. Box 217, 7500 AE Enschede, The Netherlands. r.bardin@utwente.nl

[‡]Department of Applied Mathematics, University of Twente, P.O. Box 217, 7500 AE Enschede, The Netherlands. m.schlottbom@utwente.nl

Analytic solutions to the RTE exist for simple cases only, and in general, the solution φ must be approximated by numerical methods. Classical numerical methods, such as the spherical harmonics method and the discrete ordinates method [15], approximate φ by functions of the form

$$(1.3) \quad \sum_{j=1}^J \sum_{n=1}^N \varphi_{j,n} \psi_j(\mathbf{r}) H_n(\mathbf{s}),$$

where $\{\psi_j\}$ and $\{H_n\}$ represent systems of basis functions for $H^1(D)$ and $L^2(S)$, respectively. If D and S are partitioned by quasi-uniform triangulations with a mesh size parameter h , we obtain $J \sim h^{-d}$ and $N \sim h^{-d+1}$. Hence storage of the approximate solution is proportional to $\mathcal{O}(h^{-2d+1})$, which becomes prohibitively expensive already for moderate h . We note that generally, good approximations require small h due to the hyperbolic nature of (1.1) as well as the form of the boundary condition (1.2).

The dimensionality issue leading to this unfavorable scaling has been widely addressed in literature on the RTE. In sparse tensor product methods [20, 21, 33], the essential idea is to replace the full set of indices (j, n) with $1 \leq j \leq J$ and $1 \leq n \leq N$ in (1.3) by a much smaller subset of indices (j, n) with $1 \leq f(j, n) \leq J$ for some cut-off function f . The general convergence analysis of these methods, however, requires strong smoothness assumptions on the solution, which are not guaranteed by the smoothing properties of (1.1). Moreover, either scattering [20, 33] or the boundary condition (1.2) are not fully taken into account [21]. Another class of methods constructs non-tensor product approximations. For example, [22] employs triangulations of the phase-space $D \times S$, where to each spatial element a separate triangulation of S is constructed, and the solution is then approximated by a discontinuous Galerkin method. For a simplified geometry, a discontinuous Galerkin method for arbitrary triangulations of the phase-space has been developed in [8]. In [12] the opposite approach is taken and to every discrete direction $\mathbf{s} \in S$, a spatial grid is constructed using an adaptive Petrov-Galerkin method. While this approach has a strong theoretical foundation, the practical implementation is challenging, and was done only for a small number of discrete directions \mathbf{s} and for transport dominated problems. For time-dependent problems and $d \in \{1, 2\}$, a dynamical low-rank approximation method is investigated in [28]; a related rank-adaptive integrator is developed in [23].

In this paper we propose to address the dimensionality issue for the stationary RTE by developing a low-rank tensor product framework. In order to convey the main ideas and to provide a rigorous analysis, we work with a particular quasi-one-dimensional setting, the *slab* or *plane-parallel geometry*, which amounts to a fully three-dimensional problem with symmetries [15]. In this context, $D = \mathbb{R}^2 \times (0, Z)$, with $Z > 0$ denoting the thickness of the slab, and the specific intensity $\varphi = \varphi(z, \mu)$ depends only on the spatial coordinate $z \in (0, Z)$ and on the cosine μ of the polar angle of a unit vector $\mathbf{s} \in S$. Moreover, we assume isotropic scattering $k(\mathbf{s} \cdot \mathbf{s}') = \text{const}$ and that the scattering and absorption coefficients depend on z only. In this setting, (1.1) is equivalent to the even-parity or second-order form [8, 16]

$$(1.4) \quad -\partial_z \left(\frac{\mu^2}{\sigma_t(z)} \partial_z u(z, \mu) \right) + \sigma_t(z) u(z, \mu) = \sigma_s(z) \int_0^1 u(z, \mu') d\mu' + q(z, \mu)$$

for (z, μ) in the slab $\Omega := (0, Z) \times (0, 1)$, complemented with Robin boundary conditions

$$(1.5) \quad u(z, \mu) + \frac{\mu}{\sigma_t(z)} \partial_n u(z, \mu) = g(z, \mu) \quad \text{on } \partial\Omega_- := \Gamma_0 \cup \Gamma_Z,$$

where $\Gamma_z := \{z\} \times (0, 1)$, for the even part $u(z, \mu) = \frac{1}{2}[\varphi(z, \mu) + \varphi(z, -\mu)]$. The normal derivative $\partial_n u(z, \mu)$ reads $\partial_n u(0, \mu) = -\partial_z u(0, \mu)$ and $\partial_n u(Z, \mu) = \partial_z u(Z, \mu)$.

In view of (1.3), with φ replaced by its even part u , we introduce the matrix $\mathbf{U} = [u_{j,n}]_{j,n} \in \mathbb{R}^{J \times N}$. By a standard weak formulation of the second-order equation (1.4)–(1.5), cf. [27], and Galerkin projection, we obtain a linear equation for $\mathbf{u} = \text{vec}(\mathbf{U})$,

$$(1.6) \quad \mathbb{E}\mathbf{u} = \mathbf{b},$$

where $\mathbf{b} = \text{vec}(\mathbf{B})$ denotes the load vector obtained from integrating the data q and g against the basis functions $\{\psi_j \otimes H_n\}$. We mention that the vec operation consists in stacking column-wise the elements of \mathbf{U} . Furthermore, \mathbb{E} is a fourth-order tensor of the form

$$(1.7) \quad \mathbb{E} = \sum_{l=1}^4 \mathbf{A}_l \otimes \mathbf{B}_l,$$

with matrices $\mathbf{A}_l \in \mathbb{R}^{N \times N}$ and $\mathbf{B}_l \in \mathbb{R}^{J \times J}$. Instead of forming \mathbb{E} , one usually only stores \mathbf{A}_l and \mathbf{B}_l for $1 \leq l \leq 4$. In many situations, the matrices \mathbf{A}_l and \mathbf{B}_l are either sparse or low-rank. In this case, the memory complexity for storing the components of \mathbb{E} scales like $\mathcal{O}(J + N)$.

Our aim is to construct approximations of u which have similar memory complexity and which can be computed in $\mathcal{O}(J + N)$ operations. To do so, we seek \mathbf{U} with the representation

$$(1.8) \quad \mathbf{U} = \sum_{k=1}^r \mathbf{v}_k \otimes \mathbf{w}_k \quad \text{with } \mathbf{v}_k \in \mathbb{R}^J, \mathbf{w}_k \in \mathbb{R}^N \text{ for } 1 \leq k \leq r.$$

The storage requirement for \mathbf{U} is thus $\mathcal{O}(r(J + N))$. If r is much smaller than J and N , then the representation (1.8) has much lower memory requirements than (1.3), which is of order $\mathcal{O}(JN)$. Since \mathbb{E} is not formed explicitly, we aim to solve (1.6) iteratively. The application of \mathbb{E} to \mathbf{U} is

$$(1.9) \quad \mathbb{E}\mathbf{U} := \text{mat}(\mathbb{E}\text{vec}(\mathbf{U})) = \sum_{k=1}^r \sum_{l=1}^4 (\mathbf{B}_l \mathbf{v}_k) \otimes (\mathbf{A}_l \mathbf{w}_k),$$

and the result has again storage requirements $\mathcal{O}(r(J + N))$. However, in general, the rank of the resulting matrix is increased from r to $4r$. In order to prevent uncontrolled growth of the ranks in the iterative process, we will use (i) a preconditioned iteration such that the iteration count is uniform in the size of the discretization, and (ii) a suitable rank truncation technique. See [6, 7] for similar constructions for high-dimensional elliptic problems that rely on these two core elements.

To address (i) and (ii), as in [6] we consider the symmetrically preconditioned equation

$$(1.10) \quad \mathbb{P}^{-1/2} \mathbb{E} \mathbb{P}^{-1/2} \mathbf{w} = \mathbb{P}^{-1/2} \mathbf{b},$$

with new variable $\mathbf{w} = \mathbb{P}^{1/2} \mathbf{u}$ and preconditioner \mathbb{P} . If \mathbb{P} is spectrally equivalent to \mathbb{E} , then the energy norm of the Galerkin solution to (1.4)–(1.5) is equivalent to the Euclidean norm of \mathbf{w} , i.e., using the matricizations,

$$(1.11) \quad \|\mathbf{U}\|_{\mathbb{E}}^2 := \text{trace}(\mathbf{U}^T \mathbb{E} \mathbf{U}) \approx \text{trace}(\mathbf{U}^T \mathbb{P} \mathbf{U}) = \text{trace}(\mathbf{W}^T \mathbf{W}) = \|\mathbf{W}\|_{\mathbb{F}}^2.$$

Therefore, rigorous low-rank approximations to \mathbf{U} in the energy norm can be obtained from low-rank approximations of \mathbf{W} in the Frobenius norm. In this work, we will employ established rank control

techniques based on soft thresholding of the singular values of \mathbf{W} from [7]. With thresholding parameters $\delta_k > 0$ and \mathcal{S}_{δ_k} the corresponding soft thresholding operator, we thus consider the iterative scheme

$$(1.12) \quad \mathbf{W}_{k+1} = \mathcal{S}_{\delta_k}(\mathbf{W}_k - \omega_k(\mathbb{P}^{-1/2}\mathbb{E}\mathbb{P}^{-1/2}\mathbf{W}_k - \mathbf{F})),$$

where $\mathbf{F} = \text{mat}(\mathbb{P}^{-1/2}\mathbf{b})$ and $\omega_k > 0$ is a suitable step-size parameter.

It remains to discuss the construction of a suitable preconditioner \mathbb{P} . Using a transformation of the basis $\{\psi_j \otimes H_n\}$, we show that \mathbb{E} is spectrally equivalent to a symmetric positive definite matrix with Kronecker sum structure. For such matrices, inverse powers can be approximated efficiently by exponential sum approximations [9, 30, 34]. As a result, we obtain a preconditioner \mathbb{P} such that $\mathbb{P}^{-1/2}$ is a short sum of Kronecker products similar to (1.7). The structure of the equation in slab geometry, together with our construction of the preconditioner and the setting of the Richardson iteration in the \mathbf{W} variable, allows us to use results obtained in [7] for elliptic problems to analyze (1.12). In addition to study the convergence of the scheme (1.12), following [7] we can establish upper and lower bounds for the distance between the Galerkin solution and the fixed point of (1.12), and since in general the decay behaviour of the singular values of the fixed point is unknown, we provide an algorithm which adjusts the thresholding parameter *a posteriori*. This is done based on the current iterate, retaining quasi-optimal ranks throughout the process.

The outline of the manuscript is as follows. In Section 2 we will recall the weak formulation of (1.4)–(1.5), and a choice of basis that leads to (1.6) with the corresponding representation of the operator as in (1.7). In Section 3 we discuss in detail the construction of the preconditioner \mathbb{P} . In Subsection 4.1 we then discuss different choices for \mathcal{S}_{δ_k} and state the main convergence results. Section 5 contains numerical experiments for established discretization schemes, such as truncated spherical harmonics expansions or piecewise constant approximations in μ , which show the potential of the method. We conclude the manuscript in Section 6 with some comments on possible future work.

2. Weak formulation and Galerkin approximation of the even-parity equations.

2.1. Function spaces. To introduce the weak formulation of (1.4)–(1.5), denote $L^2(\Omega)$ the usual Hilbert space of square-integrable functions with inner product (\cdot, \cdot) and induced norm $\|\cdot\|$. Furthermore, we define the Hilbert space

$$(2.1) \quad W^2(\Omega) := \{v \in L^2(\Omega) : \mu\partial_z v \in L^2(\Omega)\},$$

with norm induced by the inner product

$$(2.2) \quad (v, w)_{W^2(\Omega)} := (\mu\partial_z v, \mu\partial_z w) + ((1 + \mu^2)v, w), \quad v, w \in W^2(\Omega).$$

Since $1 \leq 1 + \mu^2 \leq 2$, we note that $\|\cdot\|_{W^2(\Omega)}$ is equivalent to the graph norm given by $\|\cdot\|_{W^2(\Omega)}^2 := \|\cdot\|^2 + \|\mu\partial_z \cdot\|^2$. The notation $\|\cdot\|_\infty$ is used for the L^∞ -norm in the z -variable. In order to incorporate boundary conditions, let us define the set $\partial\Omega_- := \Gamma_0 \cup \Gamma_Z$ with $\Gamma_z := \{z\} \times (0, 1)$ and denote $L^2(\partial\Omega_-; \mu)$ the corresponding Hilbert space of square-integrable functions with inner product denoted by $(\mu \cdot, \cdot)_{\partial\Omega_-}$. We have the following trace lemma [1, Theorem 2.8, p.55].

LEMMA 2.1. *There exists a bounded linear operator $\tau : W^2(\Omega) \rightarrow L^2(\partial\Omega_-; \mu)$, which satisfies*

$$(2.3) \quad \|\tau v\|_{L^2(\partial\Omega_-; \mu)} \leq C_{\text{tr}} \|v\|_{W^2(\Omega)} \leq C_{\text{tr}} \|v\|_{W^2(\Omega)}$$

for any $v \in W^2(\Omega)$ and $C_{\text{tr}} := 2/\sqrt{1 - \exp(-2Z)}$. Moreover, τv can be identified with $\tau_0 v = v(0, \cdot)$ and $\tau_Z v = v(Z, \cdot)$ if $v \in C^0(\bar{\Omega})$.

2.2. Weak formulation. Following the usual procedure (see, e.g., [27]) in our context, we can rewrite (1.4)–(1.5) in weak form as follows: *find* $u \in W^2(\Omega)$ *such that*

$$(2.4) \quad a_E(u, v) = b(v) \quad \text{for all } v \in W^2(\Omega),$$

with bilinear form $a_E : W^2(\Omega) \times W^2(\Omega) \rightarrow \mathbb{R}$ and linear form $b : W^2(\Omega) \rightarrow \mathbb{R}$ defined by

$$(2.5) \quad a_E(u, v) := \left(\frac{\mu^2}{\sigma_t} \partial_z u, \partial_z v \right) + (\sigma_t u, v) - (\sigma_s \mathcal{S}u, v) + (\tau u, \tau v)_{L^2(\partial\Omega_-; \mu)},$$

$$(2.6) \quad b(v) := (q, v) + (g, v)_{L^2(\partial\Omega_-; \mu)}.$$

Here $\mathcal{S} : L^2(0, 1) \rightarrow L^2(0, 1)$ denotes the μ -averaging (scattering) operator defined by

$$(2.7) \quad (\mathcal{S}v)(\mu) := \int_0^1 v(\mu') d\mu'.$$

For $v \in L^2(\Omega)$, we also write $(\mathcal{S}v)(z, \mu) := (\mathcal{S}v(z, \cdot))(\mu)$. The following hypotheses on the source terms and the optical parameters are natural in practical applications.

- Assumption 2.2.* (i) The source terms satisfy $q \in L^2(\Omega)$ and $g \in L^2(\Gamma; \mu)$.
(ii) The optical parameters satisfy $0 \leq \sigma_s, \sigma_t \in L^\infty(0, Z)$ and there exists a constant $c_0 > 0$ such that $c_0 \leq \sigma_t - \sigma_s$.

Well-posedness of (2.4) follows from standard arguments, see, e.g., [27]. We give a proof to make the constants explicit.

LEMMA 2.3. *If Assumption 2.2(ii) holds, then any $v \in W^2(\Omega)$ satisfies*

$$\gamma_1 \|v\|_{W^2(\Omega)}^2 \leq a_E(v, v) \leq \gamma_2 \|v\|_{W^2(\Omega)}^2$$

with $\gamma_1 := \min\{\|\sigma_t\|_\infty^{-1}, c_0/2\}$ and $\gamma_2 := \max\{\|\sigma_t^{-1}\|_\infty, \|\sigma_t\|_\infty, C_{\text{tr}}^2\}$, where the trace constant C_{tr} is defined in Lemma 2.1.

Proof. Using that $\sigma_t - \sigma_s \geq c_0$ by Assumption 2.2(ii), we obtain that

$$\begin{aligned} a_E(v, v) &= \left(\frac{\mu^2}{\sigma_t} \partial_z v, \partial_z v \right) + (\sigma_t v, v) - (\sigma_s \mathcal{S}v, v) + (\tau v, \tau v)_{L^2(\Gamma; \mu)} \\ &\geq \frac{1}{\|\sigma_t\|_\infty} \|\mu \partial_z v\|^2 + c_0 \|v\|^2 \geq \frac{1}{\|\sigma_t\|_\infty} \|\mu \partial_z v\|^2 + \frac{c_0}{2} \left\| \sqrt{1 + \mu^2} v \right\|^2, \end{aligned}$$

which shows the first inequality in the statement. For the second inequality, we employ Lemma 2.1 and obtain that

$$\begin{aligned} a_E(v, v) &= \left(\frac{\mu^2}{\sigma_t} \partial_z v, \partial_z v \right) + (\sigma_t v, v) - (\sigma_s \mathcal{S}v, v) + (\tau v, \tau v)_{L^2(\Gamma; \mu)} \\ &\leq \|1/\sigma_t\|_\infty \|\mu \partial_z v\|^2 + \|\sigma_t\|_\infty \left\| \sqrt{1 + \mu^2} v \right\|^2 + C_{\text{tr}}^2 \|v\|_{W^2(\Omega)}^2. \quad \square \end{aligned}$$

LEMMA 2.4. *Let Assumption 2.2 hold. Then there exists a unique $u \in W^2(\Omega)$ satisfying (2.4).*

Remark 2.5. The variational formulation (2.4) can be restated as an operator equation with differential operator $\mathcal{E} : W^2(\Omega) \rightarrow W^2(\Omega)'$ defined by the relation

$$\langle \mathcal{E}v, w \rangle = a_E(v, w) \quad \text{for all } v, w \in W^2(\Omega).$$

Here, $W^2(\Omega)'$ denotes the dual space of $W^2(\Omega)$. Note that \mathcal{E} is a short-sum of tensor products, i.e.

$$(2.8) \quad \mathcal{E} = \mu^2 \otimes \partial'_z (\Sigma_t^{-1} \partial_z) + \mathcal{I}_\mu \otimes \Sigma_t - \mathcal{S} \otimes \Sigma_s + \mu \otimes (\tau'_0 \tau_0 + \tau'_Z \tau_Z),$$

where $\partial'_z : L^2(0, Z) \rightarrow H^1(0, Z)'$ is defined by $\partial'_z : u \mapsto (u, \partial_z \cdot)_{L^2(0, Z)}$. Here $H^1(0, Z)$ denotes the usual Sobolev space. Moreover, Σ_t, Σ_s are the multiplication operators $L^2(0, Z) \rightarrow L^2(0, Z)$ defined by $u \mapsto \sigma_t u$ and $u \mapsto \sigma_s u$. [Lemma 2.3](#) can be interpreted as the spectral equivalence of \mathcal{E} and the operator $\mathcal{J} : W^2(\Omega) \rightarrow W^2(\Omega)'$ defined by

$$\langle \mathcal{J}v, w \rangle = (v, w)_{W^2(\Omega)} \quad \text{for all } v, w \in W^2(\Omega).$$

\mathcal{J} exhibits a sum of tensor products structure

$$(2.9) \quad \mathcal{J} = \mu^2 \otimes \partial'_z \partial_z + (1 + \mu^2) \otimes \mathcal{I}_z = \mu^2 \otimes (\partial'_z \partial_z + \mathcal{I}_z) + \mathcal{I}_\mu \otimes \mathcal{I}_z,$$

with \mathcal{I}_i , $i = z, \mu$, denoting the identity operator in $L^2(0, Z)$ and $L^2(0, 1)$, respectively. The second representation will be useful below, because $\partial'_z \partial_z + \mathcal{I}_z : H^1(0, Z) \rightarrow H^1(0, Z)'$ is boundedly invertible, and thus the operator \mathcal{J} is a candidate for a preconditioner for \mathcal{E} .

2.3. Galerkin approximation. We define the tensor product approximation space

$$(2.10) \quad W_{J,N}^2 = W_J^z \otimes W_N^\mu = \left\{ v_{J,N} \in W^2(\Omega) : v_{J,N}(z, \mu) = \sum_{j=1}^J \sum_{n=1}^N v_{j,n} \psi_j(z) H_n(\mu) \right\} \subset W^2(\Omega),$$

where $\{\psi_j(z)\}_{j=1}^J$ and $\{H_n(\mu)\}_{n=1}^N$ denote the sets of basis functions in space and angle, respectively. The Galerkin approximation of (2.7) then reads: *find* $u_{J,N} \in W_{J,N}^2$ *such that*

$$(2.11) \quad a_E(u_{J,N}, v_{J,N}) = b(v_{J,N}) \quad \text{for all } v_{J,N} \in W_{J,N}^2.$$

Since the bilinear form a_E is symmetric and coercive on $W^2(\Omega)$ and $W_{J,N}^2 \subset W^2(\Omega)$, standard arguments imply the following result.

LEMMA 2.6. *Let [Assumption 2.2](#) hold. Then there exists a unique solution $u_{J,N} \in W_{J,N}^2$ of (2.11). Moreover, the quasi-best approximation error estimate*

$$\|u - u_{J,N}\|_{W^2(\Omega)} \leq \frac{\gamma_2}{\gamma_1} \inf_{v_{J,N} \in W_{J,N}^2} \|u - v_{J,N}\|_{W^2(\Omega)}$$

holds, with γ_1, γ_2 from [Lemma 2.3](#).

As usual, we identify a function $u \in W_{J,N}^2$ with its coefficients $\{u_{j,n}\}$, $j = 1, \dots, J$ and $n = 1, \dots, N$, which we collect in a matrix $\mathbf{U} \in \mathbb{R}^{J \times N}$. Accordingly, we denote by $\mathbf{u} = \text{vec}(\mathbf{U}) \in \mathbb{R}^{JN}$ the vectorization of \mathbf{U} , which we obtain by stacking the columns of \mathbf{U} into a column vector. We will also write $\mathbf{U} = \text{mat}(\mathbf{u})$ for the reverse operation (matricization). The Galerkin approximation (2.11) is equivalent to the linear system

$$(2.12) \quad \mathbb{E} \mathbf{u} = \mathbf{b}$$

with matrix $\mathbb{E} \in \mathbb{R}^{JN \times JN}$. Let us give some details on the structure of \mathbb{E} .

2.4. Structure of system matrix. For coefficient functions $\nu(z)$ and $\eta(\mu)$, we define matrices $\mathbf{D}(\nu)$, \mathbf{M}_z , \mathbf{B} , \mathbf{M}_μ and \mathbf{S} by their entries for $i, j \in \{1, \dots, J\}$ and $m, n \in \{1, \dots, N\}$ as

$$\begin{aligned} [\mathbf{D}(\nu)]_{i,j} &:= \int_0^Z \nu(z) \partial_z \psi_j(z) \partial_z \psi_i(z) dz, \\ [\mathbf{M}_z(\nu)]_{i,j} &:= \int_0^Z \nu(z) \psi_j(z) \psi_i(z) dz, \\ [\mathbf{B}]_{i,j} &:= \psi_j(Z) \psi_i(Z) + \psi_j(0) \psi_i(0) \\ [\mathbf{M}_\mu(\eta)]_{m,n} &:= \int_0^1 \eta(\mu) H_m(\mu) H_n(\mu) d\mu, \\ [\mathbf{S}]_{m,n} &:= \int_0^1 (\mathcal{S}H_n) H_m d\mu. \end{aligned}$$

We write $\mathbf{D} = \mathbf{D}(1)$ and $\mathbf{M}_l = \mathbf{M}_l(1)$ for $l = z, \mu$. Using Fubini's theorem, we obtain the identity

$$(2.13) \quad \mathbb{E} = \mathbf{M}_\mu(\mu^2) \otimes \mathbf{D}(\sigma_t^{-1}) + \mathbf{M}_\mu \otimes \mathbf{M}_z(\sigma_t) - \mathbf{S} \otimes \mathbf{M}_z(\sigma_s) + \mathbf{M}_\mu(\mu) \otimes \mathbf{B}.$$

Thus \mathbb{E} is a short sum of Kronecker products, cf. (1.7) and (2.8). If \mathbf{U} has the form (1.8), we also apply \mathbb{E} to matrices and write $\mathbb{E}\mathbf{U}$ with slight abuse of notation, as defined by (1.9).

2.5. Matrix representation for the Riesz map. For notational convenience, let us make the assumption that $\{\psi_j\}_{j=1}^J$ is an orthonormal basis in $H^1(0, Z)$ and that $\{H_n\}_{n=1}^N$ is orthonormal in $L^2(0, 1)$; see Remark 2.7 for the general case. Then \mathcal{J} has the matrix representation

$$(2.14) \quad \mathbb{J} = \mathbf{M}_\mu(\mu^2) \otimes \mathbf{I}_z + \mathbf{I}_\mu \otimes \mathbf{M}_z.$$

The particular structure on the right-hand side of (2.14) is called a Kronecker sum. As an immediate consequence of Lemma 2.3, we have the spectral equivalence of \mathbb{E} and \mathbb{J} , i.e.,

$$(2.15) \quad \gamma_1 \langle \mathbb{J}\mathbf{v}, \mathbf{v} \rangle \leq \langle \mathbb{E}\mathbf{v}, \mathbf{v} \rangle \leq \gamma_2 \langle \mathbb{J}\mathbf{v}, \mathbf{v} \rangle \quad \text{for all } \mathbf{v} \in \mathbb{R}^{JN}.$$

Introducing the new variable $\mathbf{w} = \mathbb{J}^{1/2}\mathbf{u}$, (2.15) becomes

$$(2.16) \quad \gamma_1 \|\mathbf{w}\|_2^2 \leq \|u_{J,N}\|_{W^2(\Omega)}^2 \leq \gamma_2 \|\mathbf{w}\|_2^2$$

for all $u_{J,N} \in W_{J,N}^2$ with coefficient vector $\mathbf{u} \in \mathbb{R}^{JN}$. We thus have control of the Hilbert space norm of $u_{J,N}$ in terms of the Euclidean norm of \mathbf{w} .

Remark 2.7 (Change of basis). In case $\{\psi_j\}$ or $\{H_n\}$ are not orthonormal, we consider Cholesky factorizations of the Gram matrices, $\mathbf{D} + \mathbf{M}_z = \mathbf{T}_z \mathbf{T}_z^T$ and $\mathbf{M}_\mu = \mathbf{T}_\mu \mathbf{T}_\mu^T$, and observe that the representation of \mathcal{J} in that basis can be rewritten as

$$\mathbf{M}_\mu(\mu^2) \otimes (\mathbf{D} + \mathbf{M}_z) + \mathbf{M}_\mu \otimes \mathbf{M}_z = (\mathbf{T}_\mu \otimes \mathbf{T}_z) \left(\hat{\mathbf{M}}_\mu(\mu^2) \otimes \mathbf{I}_z + \mathbf{I}_\mu \otimes \hat{\mathbf{M}}_z \right) (\mathbf{T}_\mu \otimes \mathbf{T}_z)^T.$$

Therefore, up to the change of basis implied by $(\mathbf{T}_\mu \otimes \mathbf{T}_z)$, the structure of the matrix representation of \mathcal{J} is as in (2.14).

3. Preconditioning via exponential sums approximations. We next construct approximations of inverse powers of \mathbb{J} using approximations of functions $\Phi_\beta(t) := t^{-\beta}$, $\beta > 0$, by a finite series of exponentials in combination with spectral calculus. As described in [30] (see also [9] and the overview in [5]), such approximations can be obtained by discretizing integral representations of $\Phi_\beta(t)$ based on the Gamma function

$$\Gamma(z) = \int_0^{+\infty} e^{-\tau} \tau^{z-1} d\tau, \quad \operatorname{Re}(z) > 0.$$

Observe that in the definition above, z denotes a generic complex number. As shown in [30, Lemma 5.1], we have for $t > 0$ and $\operatorname{Re}(z) > 0$ the identity

$$\Gamma(z) = t^z \int_{\mathbb{R}} \exp(-te^\tau + z\tau) d\tau.$$

Therefore, we have, for any real $\beta > 0$, the representation

$$(3.1) \quad \Phi_\beta(t) = \frac{1}{\Gamma(\beta)} \int_{\mathbb{R}} \exp(-te^\tau + \beta\tau) d\tau,$$

with rapidly decaying integrand for $\tau \rightarrow \pm\infty$. Discretizing (3.1) via the trapezoidal rule with step size h on the whole real line, and truncating the infinite series, we obtain the approximation

$$(3.2) \quad \Phi_\beta(t) \approx \Psi_\beta(t) := \frac{h}{\Gamma(\beta)} \sum_{k=-k_1}^{k_2} \alpha_k(\beta) \exp(-\rho_k t)$$

for $t > 0$, with $k_1, k_2 \in \mathbb{N}$, $\alpha_k(\beta) = e^{\beta k h}$ and $\rho_k = \alpha_k(1)$. Setting $\beta = 1/2$ and requiring, for any $\epsilon > 0$, the relative error bound

$$(3.3) \quad |\Phi_{1/2}(t) - \Psi_{1/2}(t)| \leq \epsilon |\Phi_{1/2}(t)| \quad \text{for } 0 < \lambda \leq t \leq \Lambda,$$

where λ, Λ denote the lower and upper bounds on the spectrum of \mathbb{J} defined in (2.14), respectively, spectral calculus yields that

$$(3.4) \quad \|(\Phi_{1/2}(\mathbb{J}) - \Psi_{1/2}(\mathbb{J}))\mathbf{v}\|_2 \leq \epsilon \|\Phi_{1/2}(\mathbb{J})\mathbf{v}\|_2 \quad \text{for all } \mathbf{v} \in \mathbb{R}^{JN}.$$

Remark 3.1. Using the structure of \mathbb{J} , we observe that each eigenvalue of \mathbb{J} is given by a sum of an eigenvalue of $\mathbf{M}_\mu(\mu^2)$ and \mathbf{M}_z . In particular $\Lambda = \|\mathbf{M}_\mu(\mu^2)\|_2 + \|\mathbf{M}_z\|_2$.

Given the exponentiation property of the Kronecker sum, i.e.,

$$(3.5) \quad \exp(\mathbf{A} \otimes \mathbf{I} + \mathbf{I} \otimes \mathbf{B}) = \exp(\mathbf{A}) \otimes \exp(\mathbf{B}),$$

valid for general matrices \mathbf{A} and \mathbf{B} , we can define our actual preconditioner using the representation

$$(3.6) \quad \mathbb{P}^{-1/2} := \Psi_{1/2}(\mathbb{J}) = \frac{h}{\sqrt{\pi}} \sum_{k=-k_1}^{k_2} \alpha_k(1/2) \exp(-\rho_k \mathbf{M}_\mu(\mu^2)) \otimes \exp(-\rho_k \mathbf{M}_z).$$

Hence $\mathbb{P}^{-1/2}$ is a sum of Kronecker products consisting of $k_1 + k_2 + 1$ terms. The following result, specializing [5, Proposition 4.7], ensures that \mathbb{P} is a suitable preconditioner for \mathbb{E} .

LEMMA 3.2. *Let $\epsilon < 1$. If (3.4) holds, then the operator $\mathbb{P} := \Psi_{1/2}(\mathbb{J})^{-2}$ is spectrally equivalent to \mathbb{E} , i.e., for all $\mathbf{v} \in \mathbb{R}^{JN}$ we have*

$$(3.7) \quad \gamma_1^\epsilon \|\mathbf{w}\|_2^2 \leq \langle \mathbb{P}^{-1/2} \mathbb{E} \mathbb{P}^{-1/2} \mathbf{w}, \mathbf{w} \rangle \leq \gamma_2^\epsilon \|\mathbf{w}\|_2^2,$$

where $\gamma_1^\epsilon = (1 - \epsilon)^2 \gamma_1$ and $\gamma_2^\epsilon = (1 + \epsilon)^2 \gamma_2$, and γ_1, γ_2 are as in Lemma 2.3.

Proof. Setting $\mathbf{v} = \mathbb{J}^{1/2} \mathbf{w}$ in (3.4) yields

$$\|(\mathbb{I} - \mathbb{P}^{-1/2} \mathbb{J}^{1/2}) \mathbf{w}\|_2 \leq \epsilon \|\mathbf{w}\|_2.$$

Then, for $\hat{\mathbb{E}} = \mathbb{J}^{-1/2} \mathbb{E} \mathbb{J}^{-1/2}$, we have that $\langle \mathbb{P}^{-1/2} \mathbb{E} \mathbb{P}^{-1/2} \mathbf{w}, \mathbf{w} \rangle = \langle \hat{\mathbb{E}} \mathbb{J}^{1/2} \mathbb{P}^{-1/2} \mathbf{w}, \mathbb{J}^{1/2} \mathbb{P}^{-1/2} \mathbf{w} \rangle$. Hence, using the spectral equivalence (2.15), we obtain that

$$\gamma_1 \|\mathbb{J}^{1/2} \mathbb{P}^{-1/2} \mathbf{w}\|_2^2 \leq \langle \mathbb{P}^{-1/2} \mathbb{E} \mathbb{P}^{-1/2} \mathbf{w}, \mathbf{w} \rangle \leq \gamma_2 \|\mathbb{J}^{1/2} \mathbb{P}^{-1/2} \mathbf{w}\|_2^2.$$

Moreover, by the triangle inequality (\mathbb{I} is the identity matrix in $\mathbb{R}^{JN \times JN}$),

$$\begin{aligned} \|\mathbb{J}^{1/2} \mathbb{P}^{-1/2} \mathbf{w}\|_2 &\leq \|(\mathbb{I} - \mathbb{P}^{-1/2} \mathbb{J}^{1/2}) \mathbf{w}\|_2 + \|\mathbf{w}\|_2 \leq (1 + \epsilon) \|\mathbf{w}\|_2, \\ \|\mathbb{J}^{1/2} \mathbb{P}^{-1/2} \mathbf{w}\|_2 &\geq \left| \|(\mathbb{I} - \mathbb{P}^{-1/2} \mathbb{J}^{1/2}) \mathbf{w}\|_2 - \|\mathbf{w}\|_2 \right| \geq (1 - \epsilon) \|\mathbf{w}\|_2, \end{aligned}$$

concluding the proof. \square

Remark 3.3. Let us comment on the choices of the parameters h, k_1, k_2 in (3.2) to ensure the bound (3.3). As shown in [9, Theorem 3], it suffices to choose $h = h(\epsilon)$ such that

$$(3.8) \quad h \leq \frac{2\pi}{\ln(3) + \beta |\ln \cos 1| + |\ln(\epsilon)|}.$$

Hence, h depends only logarithmically on ϵ , but not on Λ/λ . We note that we require only the spectral equivalence (3.7), that is, in practice it suffices to choose a fixed $\epsilon > 0$ (say, $\epsilon = 1/10$). Performing the change of variable $s = \ln t$, (3.3) amounts to requiring

$$(3.9) \quad 1 - \epsilon \leq \sum_{k=-k_1}^{k_2} \exp(-e^{kh+s} + \frac{1}{2}(kh+s)) \leq 1 + \epsilon \quad \text{for all } \ln(\lambda) \leq s \leq \ln(\Lambda).$$

Hence, k_1, k_2 depend logarithmically on λ and Λ .

4. Transformed linear system and iterative method. Using the definition of the preconditioner in (3.6), we will from now on define $\mathbb{A} = \mathbb{P}^{-1/2} \mathbb{E} \mathbb{P}^{-1/2}$ and consider the left-right preconditioned counterpart of (2.12)

$$(4.1) \quad \mathbb{A} \mathbf{w} = \mathbf{f},$$

where $\mathbf{f} = \mathbb{P}^{-1/2} \mathbf{b}$ and $\mathbf{w} = \mathbb{P}^{1/2} \mathbf{u}$, see also (1.10) in the introduction. The next result, which follows from Lemma 3.2, shows that a Richardson iteration for the system (4.1) converges for a suitable choice of the step-size parameter ω .

THEOREM 4.1. *Let $\epsilon < 1$ and γ_2^ϵ as in [Lemma 3.2](#). For any step-size parameter $\omega \in (0, 2/\gamma_2^\epsilon)$ and any $\mathbf{w}_0 \in \mathbb{R}^{JN}$ the iteration*

$$\mathbf{w}_{k+1} = \mathbf{w}_k - \omega(\mathbb{A}\mathbf{w}_k - \mathbf{f}), \quad k \geq 0,$$

converges linearly to the solution \mathbf{w} of [\(4.1\)](#). In particular, for $\omega^ = 2/(\gamma_1^\epsilon + \gamma_2^\epsilon)$ we have that*

$$\|\mathbf{w} - \mathbf{w}_k\|_2 \leq \rho^k \|\mathbf{w} - \mathbf{w}_0\|_2 \quad \text{with } \rho = \frac{\gamma_2^\epsilon - \gamma_1^\epsilon}{\gamma_2^\epsilon + \gamma_1^\epsilon}.$$

Since \mathbb{A} is composed of operators that are short sums of Kronecker products, the memory requirement of storing \mathbb{A} is $\mathcal{O}((J+N)(k_2+k_1+1))$. In the next section, we exploit the structure of \mathbb{A} to further reduce the computational complexity when applying it.

4.1. Rank controlled iteration. From the representations of [\(3.6\)](#) for $\mathbb{P}^{-1/2}$ and [\(2.13\)](#) for \mathbb{E} , we observe that the ranks of $\mathbf{W}_k = \text{mat}(\mathbf{w}_k)$ defined in [Theorem 4.3](#) will grow in each iteration by $4(k_1+k_2+1)^2$. Therefore, we next consider rank truncation based on the singular value decomposition

$$(4.2) \quad \mathbf{W} = \sum_{k=1}^R \sigma_k \mathbf{u}_k \otimes \mathbf{v}_k,$$

with $R \leq \min\{J, N\}$ denoting the rank of \mathbf{W} . Here $\sigma_k > 0$ are the singular values of \mathbf{W} , which we assume to be ordered non-increasingly, and $\{\mathbf{u}_k\}$ form an orthonormal basis of the range of \mathbf{W} , while $\{\mathbf{v}_k\}$ form an orthonormal basis for the orthogonal complement of the kernel of \mathbf{W} .

For $\delta \geq 0$, consider the soft thresholding function s_δ , which is defined for real numbers t by

$$s_\delta(t) = \text{sgn}(t) \max\{0, |t| - \delta\}.$$

The soft thresholding operator $\mathcal{S}_\delta : \mathbb{R}^{J \times N} \rightarrow \mathbb{R}^{J \times N}$ is then defined via

$$(4.3) \quad \mathcal{S}_\delta(\mathbf{W}) = \sum_{k=1}^R s_\delta(\sigma_k) \mathbf{u}_k \otimes \mathbf{v}_k.$$

The next result recalls the non-expansiveness of the soft thresholding operator with respect to the Frobenius norm; see, e.g., [\[7, Proposition 3.2\]](#) for a proof.

PROPOSITION 4.2. *For any $\mathbf{V}, \mathbf{W} \in \mathbb{R}^{J \times N}$ and $\delta \geq 0$, the operator \mathcal{S}_δ defined in [\(4.3\)](#) satisfies $\|\mathcal{S}_\delta(\mathbf{V}) - \mathcal{S}_\delta(\mathbf{W})\|_F \leq \|\mathbf{V} - \mathbf{W}\|_F$.*

Since the composition of a non-expansive map with a contraction is a contraction, with [\[7, Lemma 4.1\]](#) applied to our setting, we obtain the following result.

THEOREM 4.3. *For any $\delta > 0$, $\mathbf{W}_0 = \text{mat}(\mathbf{w}_0) \in \mathbb{R}^{J \times N}$, and ω, ρ as in [Theorem 4.1](#), the iteration*

$$(4.4) \quad \mathbf{W}_{k+1} = \mathcal{S}_\delta(\mathbf{W}_k - \omega(\mathbb{P}^{-1/2} \mathbb{A} \mathbb{P}^{-1/2} \mathbf{W}_k - \mathbf{F}))$$

has a unique fixed point \mathbf{W}^δ satisfying

$$\|\mathbf{W}_k - \mathbf{W}^\delta\|_F \leq \rho^k \|\mathbf{W}_0 - \mathbf{W}^\delta\|_F.$$

Moreover, the distance between \mathbf{W}^δ and the matricization \mathbf{W}^* of the fixed point of the non-thresholded version of (4.4) satisfies

$$(4.5) \quad (1 + \rho)^{-1} \|\mathcal{S}_\delta(\mathbf{W}^*) - \mathbf{W}^*\|_F \leq \|\mathbf{W}^\delta - \mathbf{W}^*\|_F \leq (1 - \rho)^{-1} \|\mathcal{S}_\delta(\mathbf{W}^*) - \mathbf{W}^*\|_F.$$

Theorem 4.3 shows that the error $\|\mathbf{W}^\delta - \mathbf{W}^*\|_F$ in the limit \mathbf{W}^δ of the thresholded iteration is proportional to the error of thresholding the exact solution, which will be small if δ is chosen sufficiently small in relation to the decay of the singular values of \mathbf{W}^* .

In general, instead of using a fixed thresholding parameter δ , it is useful to consider a sequence $\delta_k \rightarrow 0$ such that the value of the parameter is decreased or maintained adaptively in each iteration, balancing the need to speed up convergence with the need to keep \mathbf{W}^{δ_k} as close as possible to \mathbf{W}^* . If the decay behavior of the singular values of \mathbf{W}^* is known, then *a priori* choice rules for the sequence of thresholding parameters are proposed and analyzed in [7]. In the more practical situation where such a decay behavior is not known, or only suboptimal estimates for the decay are available, *a posteriori* choice rules as given in [7, Section 5] are more useful. In our case, we implement such dynamical method in [Algorithm 4.1](#).

Algorithm 4.1 $\mathbf{W}^\varepsilon = \text{STSolve}(\mathbb{A}, \mathbf{F}; \varepsilon)$ adapted from [7, Algorithm 2].

Require: $\delta_0 \geq \omega \|\mathbf{F}\|_F$, $\nu, \theta \in (0, 1)$, $\gamma_1^\varepsilon, \gamma_2^\varepsilon, \omega, \rho$ as in [Theorem 4.1](#)

```

1:  $\mathbf{W}_0 := 0, \mathbf{R}_0 := -\mathbf{F}, k := 0$ 
2: while  $\|\mathbf{R}_k\|_F > \gamma_1^\varepsilon \varepsilon$  do
3:    $\mathbf{W}_{k+1} := \mathcal{S}_{\delta_k}(\mathbf{W}_k - \omega \mathbf{R}_k)$ 
4:    $\mathbf{R}_{k+1} := \mathbb{A} \mathbf{W}_{k+1} - \mathbf{F}$ 
5:   if  $\|\mathbf{W}_{k+1} - \mathbf{W}_k\|_F \leq \frac{(1-\rho)\nu}{\gamma_2^\varepsilon \rho} \|\mathbf{R}_{k+1}\|_F$  then
6:      $\delta_{k+1} := \theta \delta_k$ 
7:   else
8:      $\delta_{k+1} := \delta_k$ 
9:   end if
10:   $k \leftarrow k + 1$ 
11: end while
12:  $\mathbf{W}^\varepsilon := \mathbf{W}_k$ 

```

In order to discuss the convergence behavior of [Algorithm 4.1](#), we need some notation. By density of the approximation spaces for $J, N \rightarrow \infty$, we may think of infinite sequences of singular values now. For $\varepsilon > 0$, the truncated singular value decomposition

$$(4.6) \quad \mathbf{W}^{r^*} = \sum_{k=1}^{r^*} \sigma_k \mathbf{u}_k \otimes \mathbf{v}_k$$

yields the optimal, i.e., smallest, rank $r^* = r^*(\varepsilon)$ which satisfies $\|\mathbf{W}^{r^*} - \mathbf{W}\|_F \leq \varepsilon$. We say that a family $\{\mathbf{W}^\varepsilon\}_{\varepsilon > 0}$ of approximations for \mathbf{W} has quasi-optimal ranks if there exists a constant $C > 0$ such that $\|\mathbf{W} - \mathbf{W}^\varepsilon\|_F \leq C\varepsilon$ and if the rank of \mathbf{W}^ε is bounded by $C r^*(\varepsilon)$.

For $p > 0$, the $\ell^{p, \infty}$ -norm of the sequence $\boldsymbol{\sigma} = \{\sigma_k\}$ of singular values is defined by

$$\|\boldsymbol{\sigma}\|_{\ell^{p, \infty}} := \sup_{n \in \mathbb{N}} n^{\frac{1}{p}} \sigma_n,$$

provided the expression on the right-hand side is finite. The corresponding sequence space satisfies $\ell^{p,\infty} \subset \ell^2$ for $0 < p < 2$, and $\boldsymbol{\sigma} \in \ell^{p,\infty}$ if and only if there exists $C > 0$ such that

$$\sqrt{\sum_{k>n} |\sigma_k|^2} \leq Cn^{-s} \quad \text{for } s := \frac{1}{p} - \frac{1}{2},$$

see, e.g., [13]. Therefore, $\boldsymbol{\sigma} \in \ell^{p,\infty}$ for some $0 < p < 2$ ensures algebraic decay of the singular values and the quasi-best ranks scale like $C^{1/s}\varepsilon^{-1/s}$.

The next result, whose proof carries over from the proof of [7, Theorem 5.1], ensures that the iterates produced by the algorithm are of quasi-optimal ranks.

THEOREM 4.4. *For any $\varepsilon > 0$, [Algorithm 4.1](#) produces an approximation \mathbf{W}^ε to \mathbf{W}^* with $\|\mathbf{W}^\varepsilon - \mathbf{W}^*\|_F \leq \varepsilon$ in finitely many steps. Moreover,*

- (i) *if $\boldsymbol{\sigma}^*$, the sequence of singular values of \mathbf{W}^* , satisfies $\boldsymbol{\sigma}^* \in \ell^{p,\infty}$, then there exist $\tilde{\rho} \in (0, 1)$ and a constant $C > 0$, depending on $\gamma_1^\varepsilon, \gamma_2^\varepsilon, \theta, \nu, \delta_0$ and p , such that with $\varepsilon_k := \tilde{\rho}^k$ and $s = 1/p - 1/2$, we have*

$$\|\mathbf{W}_k - \mathbf{W}^*\|_F \leq C\varepsilon_k, \quad \text{rank}(\mathbf{W}_k) \leq C^2 \|\boldsymbol{\sigma}^*\|_{\ell^{p,\infty}}^{1/s} \varepsilon_k^{-1/s};$$

- (ii) *if $\sigma_k^* \leq c_1 \exp(-c_2 k^\beta)$ for some constants $\beta, c_1, c_2 > 0$, then there exist $\tilde{\rho} \in (0, 1)$ and a constant $C > 0$, depending on $\gamma_1^\varepsilon, \gamma_2^\varepsilon, \theta, \nu, \delta_0, p, c_1, c_2$ and β , such that with $\varepsilon_k := \tilde{\rho}^k$, we have*

$$\|\mathbf{W}_k - \mathbf{W}^*\|_F \leq C\varepsilon_k, \quad \text{rank}(\mathbf{W}_k) \leq C(1 + |\ln(\varepsilon_k)|)^{1/\beta}.$$

Note that [Algorithm 4.1](#) does not require the user to specify or estimate the decay behaviour of the singular values of the solution. Hence, [Algorithm 4.1](#) automatically produces convergent iterates having quasi-optimal ranks.

5. Numerical experiments. In this section we present numerical experiments to illustrate applications of [Algorithm 4.1](#). We show that, upon mesh refinement, the final iterates have approximation errors that behave like the error of the underlying Galerkin discretization, while the ranks of the corresponding iterates remain moderately small. Before turning to the results for the thresholded Richardson iteration, we describe two discretization schemes in the next sections.

5.1. P_N -FEM method. Consider an equi-spaced partition $0 = z_0 < z_1 < \dots < z_J = Z$ of the interval $(0, Z)$, and let $\psi_j(z)$ be the piecewise linear functions on this partition such that $\psi_j(z_i) = \delta_{i,j}$. For the discretization in μ , denote by L_n the Legendre polynomial of degree n , $n < N$ and N odd, associated with the interval $(-1, 1)$. We recall that L_n is even if and only if n is even. Since we only approximate the even part of the solution, we may therefore choose H_n to be the restriction of L_{2n} to $(0, 1)$ such that $\int_0^1 H_n(\mu) H_m(\mu) d\mu = \delta_{m,n}$. Observe that with these choices, the spatial matrices have all size $(J+1) \times (J+1)$, being J the number of spatial elements in the interval $(0, Z)$; the angular matrices have size $(M+1) \times (M+1)$, with $M := (N-1)/2$. All matrices described in [Subsection 2.4](#) are sparse, except the boundary matrix $\mathbf{M}_\mu(\mu)$; see, however, [17] for a possible remedy. Furthermore, $\mathbf{M}_\mu = \mathbf{I}_\mu$. Since the Gram matrix $\mathbf{D} + \mathbf{M}_z$ of the $H^1(0, Z)$ -inner product is not diagonal, we follow the strategy outlined in [Remark 2.7](#) and perform a change of basis using the Cholesky factorization $\mathbf{D} + \mathbf{M}_z = \mathbf{T}_z \mathbf{T}_z^T$. Since $\mathbf{D} + \mathbf{M}_z$ is tridiagonal, \mathbf{T}_z can be computed and applied in $\mathcal{O}(J)$ operations. Moreover, the inverse \mathbf{T}_z^{-1} can be applied in $\mathcal{O}(J)$ operations as well. Regarding the spectral bounds λ and Λ required in [Section 3](#), we need to

estimate the smallest and largest eigenvalues of $\mathbf{M}_\mu(\mu^2)$ and $\mathbf{T}_z^{-1}\mathbf{M}_z\mathbf{T}_z^{-T}$. We have the following results:

LEMMA 5.1. *There exists $c_N > 1$, with $|1 - c_N| \sim N^{-2}$, such that*

$$c_N N^{-4} \|\mathbf{v}\|_2^2 \leq \langle \mathbf{M}_\mu(\mu^2) \mathbf{v}, \mathbf{v} \rangle \leq \|\mathbf{v}\|_2^2 \quad \forall \mathbf{v} \in \mathbb{R}^{M+1}.$$

Proof. Let $v(\mu) = \sum_{m=0}^M v_m H_m(\mu)$. Then

$$\langle \mathbf{M}_\mu(\mu^2) \mathbf{v}, \mathbf{v} \rangle = \int_0^1 |v|^2 \mu^2 d\mu \leq \int_0^1 |v|^2 d\mu = \|\mathbf{v}\|_2^2,$$

showing the upper bound. Regarding the lower bound, let $\{(\mu_k, w_k)\}$ be a Gauss-Legendre quadrature rule with $2(M+1) = N+1$ points on $(0, 1)$ and positive weights. Since the degree of exactness is $4M+3$ and $v^2 \mu^2$ has a maximal degree of $4M+2$, it follows that

$$\int_0^1 |v|^2 \mu^2 d\mu = \sum_{k=0}^{2M+2} w_k v(\mu_k)^2 \mu_k^2 \geq \min_k \mu_k^2 \int_0^1 v^2 d\mu = \min_k \mu_k^2 \|\mathbf{v}\|_2^2.$$

To complete the proof, we combine the following asymptotic formula for the integration points, see [32] or [19],

$$(5.1) \quad 2\mu_k - 1 = \left[1 - \frac{1}{8(N+1)^2} + \frac{1}{8(N+1)^3} \right] \cos \left(\pi \frac{4k-1}{4(N+1)+2} \right) + \mathcal{O}(N^{-4}),$$

with Taylor expansion of the trigonometric function. \square

LEMMA 5.2. *There exists a constant $c > 0$ independent of J such that*

$$cJ^{-2} \|\mathbf{v}\|_2^2 \leq \langle \mathbf{T}_z^{-1} \mathbf{M}_z \mathbf{T}_z^{-T} \mathbf{v}, \mathbf{v} \rangle \leq \|\mathbf{v}\|_2^2 \quad \forall \mathbf{v} \in \mathbb{R}^{J+1}.$$

Proof. Since $\mathbf{T}_z \mathbf{T}_z^T = \mathbf{D} + \mathbf{M}_z$, the eigenvalues λ of $\mathbf{T}_z^{-1} \mathbf{M}_z \mathbf{T}_z^{-T}$ satisfy

$$(\mathbf{D} + \mathbf{M}_z) \mathbf{v} = \lambda^{-1} \mathbf{v}$$

with corresponding eigenvectors \mathbf{v} . Standard inverse inequalities, see, e.g., [24, p. 85], then allow to estimate λ as asserted. \square

Remark 5.3. The previous results imply that $\Lambda \leq 2$ and $\lambda \geq c_N N^{-2} + cJ^{-2}$. Straightforward computation yields $c = 12$. For very large problems, for instance $J = 10^6$, $N = 2^{15} + 1$, we obtain an exponential sum approximation with $\epsilon = 0.1$ with 17 terms, i.e. $k_1 = 3$ and $k_2 = 13$.

5.2. S_N -FEM method. We consider the same discretization of the z -dependence as in the P_N -FEM method. In order to discretize the μ -dependence, we let $\{H_n\}$ be piecewise constant functions associated to a partition $0 = \mu_0 < \mu_1 < \dots < \mu_N = 1$ such that $H_n(\mu) = 1/\sqrt{\mu_{n+1} - \mu_n}$ for $\mu \in (\mu_n, \mu_{n+1})$ and $H_n(\mu) = 0$ else. For ease of discussion, we assume that this partition is equi-spaced with spacing $h_\mu = \mu_1 - \mu_0$. We then obtain that all matrices are sparse, except \mathbf{S} which has rank one, and that $\mathbf{M}_\mu = \mathbf{I}_\mu$. The spectral bounds $\lambda \geq c/J^2 + 1/(3N^2)$ and $\Lambda \leq 2$ can then be computed from Lemma 5.2 and the next result.

LEMMA 5.4. *Let $c_N = 1/(3N^2)$. Then we have that*

$$c_N \|\mathbf{v}\|_2^2 \leq \langle \mathbf{M}_\mu(\mu^2) \mathbf{v}, \mathbf{v} \rangle \leq \|\mathbf{v}\|_2^2 \quad \forall \mathbf{v} \in \mathbb{R}^N.$$

Proof. The claim follows from the observation that $\mathbf{M}_\mu(\mu^2)$ is diagonal, with diagonal entries \square

$$\int_0^1 \mu^2 H_n(\mu)^2 d\mu = \frac{1}{h_\mu} \int_{\mu_n}^{\mu_{n+1}} \mu^2 d\mu = \frac{1}{3}(3\mu_n^2 + 3\mu_n h_\mu + h_\mu^2).$$

Remark 5.5. A similar consideration as in [Remark 5.3](#) can be done also in this case for large problems. In general, for both P_N -FEM and S_N -FEM methods, moderate ranks of the preconditioner can be achieved.

5.3. Rank-1 manufactured solution. We fix optical parameters $\sigma_a(z) = 3$ and $\sigma_s(z) = 1 + \frac{1}{2} \sin(\pi z)$ and consider a rank-1 manufactured solution

$$(5.2) \quad \varphi_1(z, \mu) = |\mu| e^{-\mu} e^{-z(1-z)},$$

with even part $u_1(z, \mu) = |\mu| \cosh(\mu) e^{-z(1-z)}$ having also rank one. For our experiments, we employ [Algorithm 4.1](#) with initial thresholding parameter $\delta_0 = 10^{-1}$, reduction factor for the thresholding parameter $\theta = 0.75$, tolerance for the iterative method $\varepsilon = 10^{-7}$, and $\nu = 0.5$. We denote with $u_{J,N}$ the back transformation of the output of [Algorithm 4.1](#), through the preconditioner $\mathbb{P}^{-1/2}$. [Table 5.1](#) and [Table 5.2](#) show the behaviour of the L^2 - and W_G^2 -errors, together with the corresponding convergence rates upon mesh refinement, for the P_N -FEM and S_N -FEM methods, as described in [Subsection 5.1](#) and [Subsection 5.2](#). We observe that employing $N \sim J^{2/3}$ (motivated for instance in [\[17\]](#)) for the P_N method, and $N \sim J$ for the S_N method, we retain the optimal convergence rate of 1 for both error norms. Moreover, the number of iterations and the ranks of \mathbf{W}^ε (third and second-last column of [Table 5.1](#) and [Table 5.2](#)) are robust under mesh refinement. The ranks of $\mathbf{U}^\varepsilon := \mathbb{P}^{-1/2} \mathbf{W}^\varepsilon$ are bounded by product of the ranks of $\mathbb{P}^{-1/2}$ and \mathbf{W}^ε . Therefore the rank of \mathbf{U}^ε is only slightly larger than the rank of \mathbf{W}^ε , see also [Remark 3.3](#). Since the exact rank of \mathbf{U}^ε with respect to the energy norm cannot be computed, we give for comparison the rank of \mathbf{U}^ε computed in the Euclidean setting. In [Figure 5.1](#) we show the behaviour of the ranks of each iterate (left column) and of the thresholding parameter (right column) as the iterative method progresses. The mild increase in the ranks during the iteration verifies the low computational costs. In particular, there are no intermediate high ranks. We note, however, that the ranks of the corresponding Galerkin solution, which we closely approximate with the choice $\varepsilon = 10^{-7}$, and its transformation to the \mathbf{w} -variables are unknown.

Motivated by the observation that quasi-optimal ranks might be achieved if the error tolerances are not too strict, see, e.g., [\[14, Lemma 2.7\]](#), we also consider the S_N -FEM method with variable tolerance of $\varepsilon = 0.1/J$ in [Algorithm 4.1](#). As shown in [Table 5.3](#), this choice lowers both the number of iterations (which is no longer constant, but depends on the mesh) and the final rank of \mathbf{W}^ε , which remains close to the optimal rank, speeding up convergence but at the same time retaining the optimal convergence rate for both norms.

5.4. Exact solution of infinite rank. We consider now a manufactured solution with (potentially) infinite rank. The optical parameters are the same as in [Subsection 5.3](#), as well as the

TABLE 5.1

Discretization L^2 - and W_G^2 -errors, with convergence rates, and number of iterations of *Algorithm 4.1* for the P_N -FEM method applied to test case (5.2). Last two columns: final rank of the output of the algorithm and of its back transformation through the preconditioner.

P_N -FEM method, $\varepsilon = 10^{-7}$								
J	N	k	$\ u_1 - u_{J,N}\ _{L^2(\Omega)}$	rate	$\ u_1 - u_{J,N}\ _{W_G^2(\Omega)}$	rate	$\mathbf{r}(\mathbf{W}^\varepsilon)$	$\mathbf{r}(\mathbf{U}^\varepsilon)$
128	27	286	$2.72 \cdot 10^{-3}$	0.98	$4.01 \cdot 10^{-3}$	0.99	10	13
256	41	274	$1.47 \cdot 10^{-3}$	0.89	$2.08 \cdot 10^{-3}$	0.95	10	15
512	65	267	$7.41 \cdot 10^{-4}$	0.99	$1.04 \cdot 10^{-3}$	1.00	11	16
1024	103	256	$3.73 \cdot 10^{-4}$	0.99	$5.21 \cdot 10^{-4}$	0.99	11	17
2048	163	257	$1.88 \cdot 10^{-4}$	0.99	$2.61 \cdot 10^{-4}$	1.00	12	19
4096	257	247	$9.50 \cdot 10^{-5}$	0.98	$1.31 \cdot 10^{-4}$	0.99	12	20

TABLE 5.2

Discretization L^2 - and W_G^2 -errors, with convergence rates, and number of iterations of *Algorithm 4.1* for the S_N -FEM method applied to test case (5.2). Last two columns: final rank of the output of the algorithm and of its back transformation through the preconditioner.

S_N -FEM method, $\varepsilon = 10^{-7}$								
J	N	k	$\ u_1 - u_{J,N}\ _{L^2(\Omega)}$	rate	$\ u_1 - u_{J,N}\ _{W^2(\Omega)}$	rate	$\mathbf{r}(\mathbf{W}^\varepsilon)$	$\mathbf{r}(\mathbf{U}^\varepsilon)$
128	128	232	$3.12 \cdot 10^{-3}$	1.00	$4.45 \cdot 10^{-3}$	1.00	16	24
256	256	223	$1.56 \cdot 10^{-3}$	1.00	$2.23 \cdot 10^{-3}$	1.00	16	25
512	512	216	$7.79 \cdot 10^{-4}$	1.00	$1.11 \cdot 10^{-3}$	1.00	15	27
1024	1024	215	$3.81 \cdot 10^{-4}$	1.00	$5.56 \cdot 10^{-4}$	1.00	16	28

TABLE 5.3

Discretization L^2 - and W_G^2 -errors, with convergence rates, and number of iterations of *Algorithm 4.1* for the S_N -FEM method applied to test case (5.2) with Richardson tolerance chosen as $0.1/J$. Last two columns: final rank of the output of the algorithm and of its back transformation through the preconditioner.

S_N -FEM method, $\varepsilon = 0.1/J$								
J	N	k	$\ u_1 - u_{J,N}\ _{L^2(\Omega)}$	rate	$\ u_1 - u_{J,N}\ _{W^2(\Omega)}$	rate	$\mathbf{r}(\mathbf{W}^\varepsilon)$	$\mathbf{r}(\mathbf{U}^\varepsilon)$
128	128	88	$3.12 \cdot 10^{-3}$	1.00	$4.46 \cdot 10^{-3}$	1.00	3	18
256	256	98	$1.56 \cdot 10^{-3}$	1.00	$2.23 \cdot 10^{-3}$	1.00	4	20
512	512	107	$7.79 \cdot 10^{-4}$	1.00	$1.11 \cdot 10^{-3}$	1.00	4	21
1024	1024	116	$3.90 \cdot 10^{-4}$	1.00	$5.57 \cdot 10^{-4}$	1.00	4	21

setup of the iterative method. The exact solution is built through its $L^2(\Omega)$ -SVD as follows

$$(5.3) \quad \varphi(z, \mu) = u_2(z, \mu) = 2 \sum_{k=1}^{\infty} \sigma_k \sin(k\pi z) \cos(k\pi \mu).$$

For the experiments below, we choose $\sigma_k = k^{-3}$ for the algebraic behaviour (it can be proved that $\sigma \in \ell^{2/7, \infty} \subset \ell^2$ in this case), and $\sigma_k = \exp(-k^2)$ for the exponential behaviour. We observe that, as in the previous subsection, the mentioned decay rates for the singular values hold for u_2 in the $L^2(\Omega)$ -norm, but not necessarily in the graph norm. Moreover, we do not know either the behavior

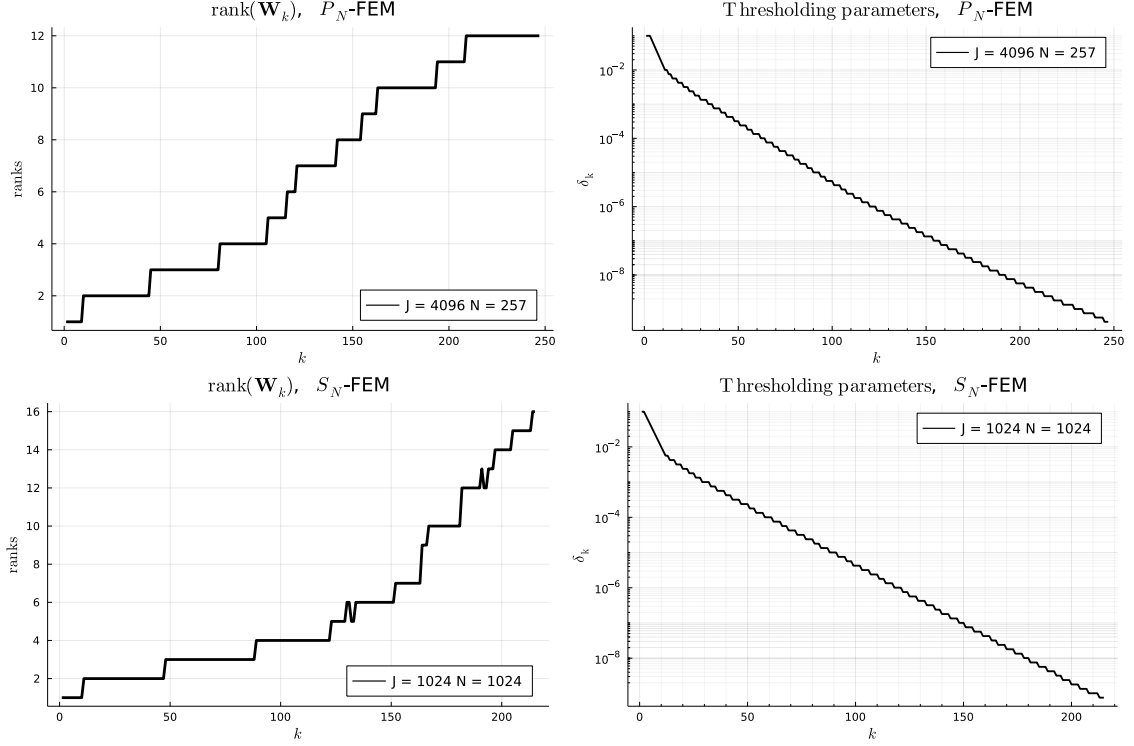


FIGURE 5.1. Behaviour of iterates ranks (left) and thresholding parameter (right) for the P_N -FEM (top) and S_N -FEM (bottom) methods applied to test case (5.2) with Richardson tolerance $\varepsilon = 10^{-7}$.

of the singular values of the corresponding transformation of u_2 under $\mathbb{P}^{1/2}$ or the corresponding behavior for the Galerkin approximation.

In Tables 5.4 and 5.5 we report the results for the P_N -FEM method. We observe optimal convergence rates for the error when J is increased. At the same time, the iteration count required for convergence with fixed tolerance $\varepsilon = 10^{-7}$ as well as the resulting ranks are robust upon mesh refinement.

The corresponding results for the S_N -FEM method are reported in Table 5.6 and Table 5.8. Similar comments as for the P_N -FEM method apply.

For the S_N -method, we report in Table 5.7 and Table 5.9 the results for an iterative scheme with tolerance dependent on the mesh, i.e. $\varepsilon = 0.1/J$; see also the previous subsection for a motivation. These results show that the same optimal convergence rates can be achieved without being too greedy on the tolerance, keeping at the same time the ranks of the iterates smaller than the cases with $\varepsilon = 10^{-7}$. Moreover, the increase in the ranks upon mesh refinement is small.

5.5. A physical problem. In this last example we test our method on a test case inspired by an imaging application. Consider an infrared beam (wavelength $\lambda_{\text{ir}} = 800$ nm) hitting the human body perpendicular to the skin surface. We assume a Gaussian-like inflow specific intensity on the

TABLE 5.4

Discretization L^2 - and W_G^2 -errors, with convergence rates, and number of iterations of *Algorithm 4.1* for the P_N -FEM method applied to test case (5.3) with $\sigma_k = k^{-3}$. Last two columns: final rank of the output of the algorithm and of its back transformation through the preconditioner.

P_N -FEM method								
J	N	k	$\ u_2 - u_{J,N}\ _{L^2(\Omega)}$	rate	$\ u_2 - u_{J,N}\ _{W^2(\Omega)}$	rate	$\mathbf{r}(\mathbf{W}^\varepsilon)$	$\mathbf{r}(\mathbf{U}^\varepsilon)$
128	27	435	$1.62 \cdot 10^{-3}$	1.61	$2.54 \cdot 10^{-2}$	1.10	14	14
256	41	447	$5.52 \cdot 10^{-4}$	1.55	$1.12 \cdot 10^{-2}$	1.18	21	21
512	65	444	$2.47 \cdot 10^{-5}$	4.48	$4.27 \cdot 10^{-3}$	1.39	27	30
1024	103	445	$8.76 \cdot 10^{-7}$	4.82	$2.13 \cdot 10^{-3}$	1.00	28	32
2048	163	445	$4.87 \cdot 10^{-7}$	0.85	$1.07 \cdot 10^{-3}$	1.00	30	34
4096	257	445	$5.92 \cdot 10^{-8}$	3.04	$5.33 \cdot 10^{-4}$	1.00	31	36

TABLE 5.5

Discretization L^2 - and W_G^2 -errors, with convergence rates, and number of iterations of *Algorithm 4.1* for the P_N -FEM method applied to test case (5.3) with $\sigma_k = \exp(-k^2)$. Last two columns: final rank of the output of the algorithm and of its back transformation through the preconditioner.

P_N -FEM method, $\varepsilon = 10^{-7}$								
J	N	k	$\ u_2 - u_{J,N}\ _{L^2(\Omega)}$	rate	$\ u_2 - u_{J,N}\ _{W^2(\Omega)}$	rate	$\mathbf{r}(\mathbf{W}^\varepsilon)$	$\mathbf{r}(\mathbf{U}^\varepsilon)$
128	27	337	$1.70 \cdot 10^{-5}$	2.00	$5.16 \cdot 10^{-3}$	1.00	11	14
256	41	335	$4.25 \cdot 10^{-6}$	2.00	$2.58 \cdot 10^{-3}$	1.00	13	17
512	65	335	$1.07 \cdot 10^{-6}$	1.99	$1.29 \cdot 10^{-3}$	1.00	13	19
1024	103	334	$2.74 \cdot 10^{-7}$	1.97	$6.46 \cdot 10^{-4}$	1.00	15	21
2048	163	333	$9.42 \cdot 10^{-8}$	1.54	$3.23 \cdot 10^{-4}$	1.00	16	23
4096	257	334	$6.75 \cdot 10^{-8}$	0.48	$1.61 \cdot 10^{-4}$	1.00	18	26

TABLE 5.6

Discretization L^2 - and W_G^2 -errors, with convergence rates, and number of iterations of *Algorithm 4.1* for the S_N -FEM method applied to test case (5.3) with $\sigma_k = k^{-3}$. Last two columns: final rank of the output of the algorithm and of its back transformation through the preconditioner.

S_N -FEM method, $\varepsilon = 10^{-7}$								
J	N	k	$\ u_2 - u_{J,N}\ _{L^2(\Omega)}$	rate	$\ u_2 - u_{J,N}\ _{W^2(\Omega)}$	rate	$\mathbf{r}(\mathbf{W}^\varepsilon)$	$\mathbf{r}(\mathbf{U}^\varepsilon)$
128	128	429	$7.37 \cdot 10^{-3}$	1.00	$2.41 \cdot 10^{-2}$	1.00	31	36
256	256	439	$3.69 \cdot 10^{-3}$	1.00	$1.21 \cdot 10^{-2}$	1.00	33	39
512	512	429	$1.84 \cdot 10^{-3}$	1.00	$6.03 \cdot 10^{-3}$	1.00	34	42
1024	1024	429	$9.21 \cdot 10^{-4}$	1.00	$3.01 \cdot 10^{-3}$	1.00	36	45

left part of the slab, vanishing on the right part, i.e.,

$$g(0, \mu) = \alpha e^{-(1-\mu)^2/\beta}, \quad g(1, \mu) = 0.$$

We assume there are no internal sources of radiation, $q \equiv 0$. Let us consider a slab of total length 20 mm constituted by three layers: skin, blood, and muscle. We choose the scattering and

TABLE 5.7

Discretization L^2 - and W_G^2 -errors, with convergence rates, and number of iterations of *Algorithm 4.1* for the S_N -FEM method applied to test case (5.3) with $\sigma_k = k^{-3}$ and Richardson tolerance adaptively chosen as $0.1/J$. Last two columns: final rank of the output of the algorithm and of its back transformation through the preconditioner.

S_N -FEM method, $\varepsilon = 0.1/J$									
J	N	k	$\ u_2 - u_{J,N}\ _{L^2(\Omega)}$	rate	$\ u_2 - u_{J,N}\ _{W^2(\Omega)}$	rate	$\mathbf{r}(\mathbf{W}^\varepsilon)$	$\mathbf{r}(\mathbf{U}^\varepsilon)$	
128	128	208	$7.37 \cdot 10^{-3}$	1.00	$2.41 \cdot 10^{-2}$	1.00	23	35	
256	256	226	$3.69 \cdot 10^{-3}$	1.00	$1.21 \cdot 10^{-2}$	1.00	25	38	
512	512	242	$1.84 \cdot 10^{-3}$	1.00	$6.03 \cdot 10^{-3}$	1.00	26	40	
1024	1024	260	$9.21 \cdot 10^{-4}$	1.00	$3.01 \cdot 10^{-3}$	1.00	27	43	

TABLE 5.8

Discretization L^2 - and W_G^2 -errors, with convergence rates, and number of iterations of *Algorithm 4.1* for the S_N -FEM method applied to test case (5.3) with $\sigma_k = \exp(-k^2)$. Last two columns: final rank of the output of the algorithm and of its back transformation through the preconditioner.

S_N -FEM method, $\varepsilon = 10^{-7}$									
J	N	k	$\ u_2 - u_{J,N}\ _{L^2(\Omega)}$	rate	$\ u_2 - u_{J,N}\ _{W^2(\Omega)}$	rate	$\mathbf{r}(\mathbf{W}^\varepsilon)$	$\mathbf{r}(\mathbf{U}^\varepsilon)$	
128	128	297	$2.62 \cdot 10^{-3}$	1.00	$7.30 \cdot 10^{-3}$	1.00	17	26	
256	256	297	$1.31 \cdot 10^{-3}$	1.00	$3.65 \cdot 10^{-3}$	1.00	19	29	
512	512	297	$6.55 \cdot 10^{-4}$	1.00	$1.83 \cdot 10^{-3}$	1.00	20	32	
1024	1024	298	$3.27 \cdot 10^{-4}$	1.00	$9.13 \cdot 10^{-4}$	1.00	22	35	

TABLE 5.9

Discretization L^2 - and W_G^2 -errors, with convergence rates, and number of iterations of *Algorithm 4.1* for the S_N -FEM method applied to test case (5.3) with $\sigma_k = \exp(-k^2)$ and Richardson tolerance adaptively chosen as $0.1/J$. Last two columns: final rank of the output of the algorithm and of its back transformation through the preconditioner.

S_N -FEM method, $\varepsilon = 0.1/J$									
J	N	k	$\ u_2 - u_{J,N}\ _{L^2(\Omega)}$	rate	$\ u_2 - u_{J,N}\ _{W^2(\Omega)}$	rate	$\mathbf{r}(\mathbf{W}^\varepsilon)$	$\mathbf{r}(\mathbf{U}^\varepsilon)$	
128	128	127	$2.62 \cdot 10^{-3}$	1.00	$7.30 \cdot 10^{-3}$	1.00	9	25	
256	256	138	$1.31 \cdot 10^{-3}$	1.00	$3.65 \cdot 10^{-3}$	1.00	9	28	
512	512	150	$6.55 \cdot 10^{-4}$	1.00	$1.83 \cdot 10^{-3}$	1.00	10	31	
1024	1024	162	$3.27 \cdot 10^{-4}$	1.00	$9.13 \cdot 10^{-4}$	1.00	12	33	

absorption parameters to be piecewise constant functions

$$(5.4) \quad \begin{aligned} \sigma_s(z) &= 36.52\chi_{[0,0.75)}(z) + 32.27\chi_{[0.75,0.875)}(z) + 5.20\chi_{[0.875,1]}(z) \\ \sigma_a(z) &= 0.52\chi_{[0,0.75)}(z) + 8.31\chi_{[0.75,0.875)}(z) + 0.60\chi_{[0.875,1]}(z), \end{aligned}$$

which reflects realistic width for the layers (~ 15 mm for skin, ~ 2.5 mm for blood and ~ 2.5 mm for muscle), cf., e.g., [3]. Given this construction and following [35], realistic values for α and β are $\alpha = 2.4$ and $\beta = 2500$. For this test case no analytic solution is available. However, due to the strong concentration of the source term g around $\mu = 1$, we expect a high value of N is required in the P_N -FEM method to obtain accurate solutions. We run our algorithm with a Richardson

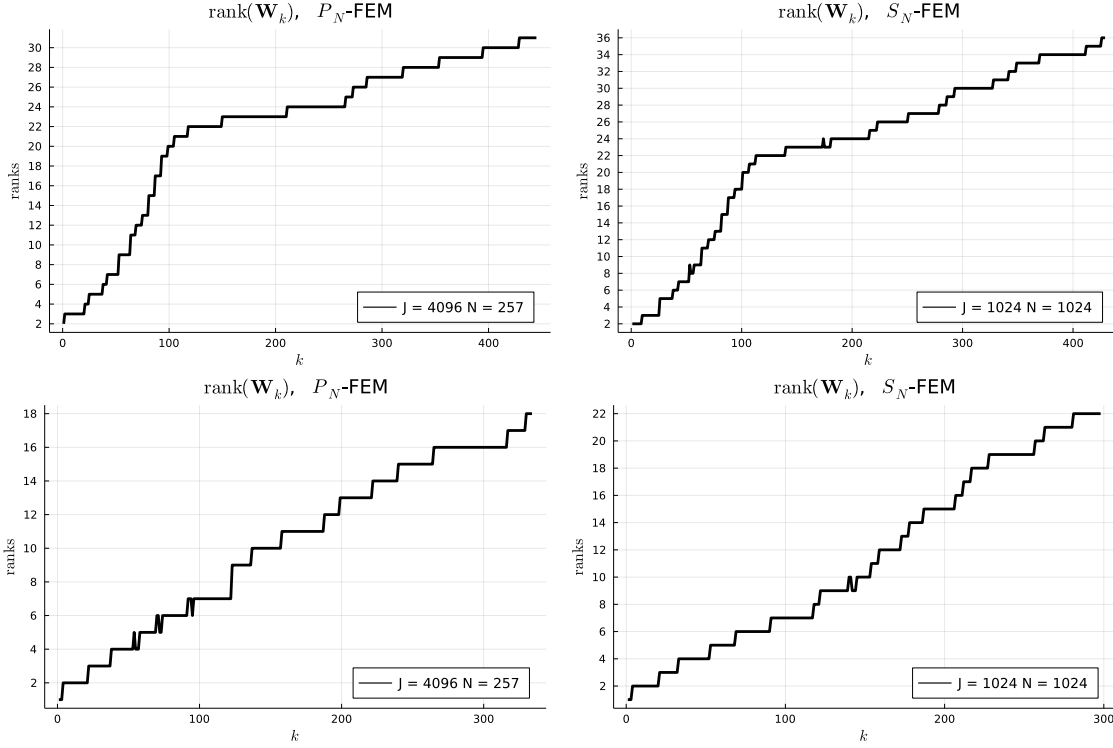


FIGURE 5.2. Behaviour of iterates ranks for the P_N -FEM and S_N -FEM methods applied to test case (5.3) with algebraic (top row) and exponential (bottom row) decay of the singular values.

tolerance set to $\varepsilon = 10^{-4}$. As shown in Table 5.10 and in the top-left plots of Figure 5.3 and Figure 5.4, we confirm the ability of our method to keep the ranks of the iterates small during the procedure. Decay of the residuals (bottom-left plots) allows to control the convergence of the method. The bottom-right plots show the decay of the singular values of the output \mathbf{W}^ε , as well as the one of its back-transformed $u_{J,N}$ through the preconditioner.

TABLE 5.10

Number of iterations of Algorithm 4.1 for the P_N -FEM (left) and S_N -FEM (right) methods applied to test case (5.4), and final rank of the output of the algorithm and of its back transformation through the preconditioner.

P_N -FEM method					S_N -FEM method				
J	N	k	$\mathbf{r}(\mathbf{W}^\varepsilon)$	$\mathbf{r}(\mathbf{U}^\varepsilon)$	J	N	k	$\mathbf{r}(\mathbf{W}^\varepsilon)$	$\mathbf{r}(\mathbf{U}^\varepsilon)$
128	27	15154	12	14	128	128	13857	15	33
256	41	15553	13	21	256	256	14041	17	37
512	65	15591	14	26	512	512	14147	18	40
1024	103	15698	15	29	1024	1024	14236	19	44
2048	163	15805	17	31					
4096	257	15792	18	35					

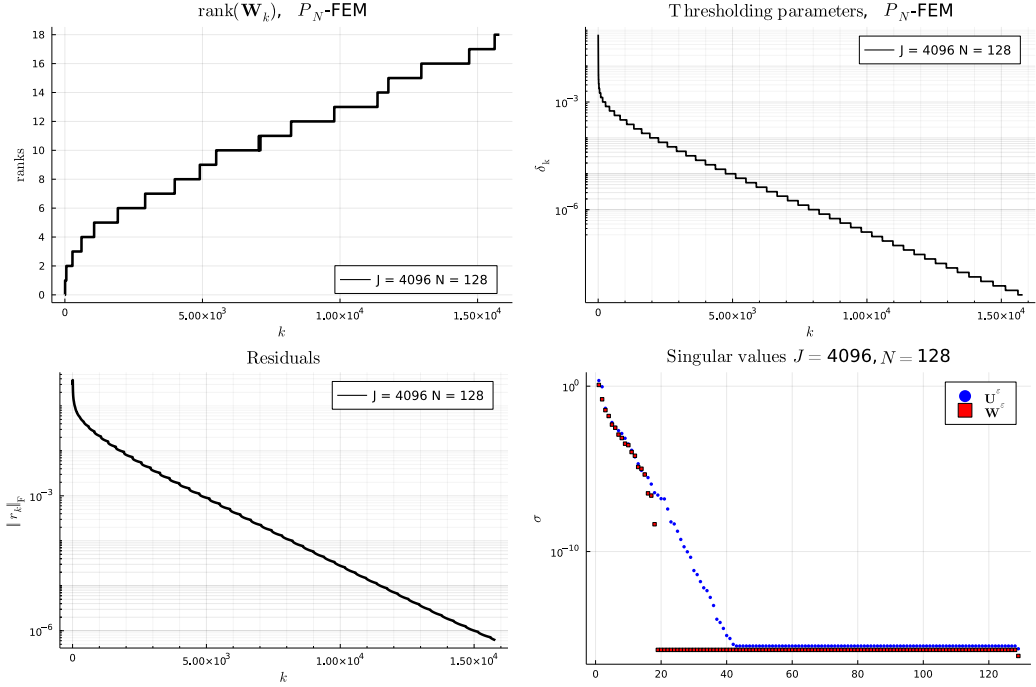


FIGURE 5.3. Behaviour of iterates ranks (top left), thresholding parameter (top right), Frobenius norm of the residuals (bottom left) and singular values of both \mathbf{W}^ε and \mathbf{U}^ε (bottom right), for the P_N -FEM method applied to test case (5.4).

6. Conclusions and possible extensions. We have developed a rigorous low-rank framework for the even-parity formulation of the stationary monochromatic radiative transfer equation in slab geometry, which can be applied to many discretization schemes as exemplified by considering widely used P_N and S_N schemes. Our framework employs iterative computations that efficiently maintain low ranks for the iterates. To keep the total number of iterations low, we have devised a preconditioner in Kronecker-sum format that is based on exponential sum approximations. Moreover, the preconditioner allows control over errors in energy norm by performing computations in corresponding Euclidean spaces. For the exemplary considered discretizations, we made all hyperparameters, such as choice of the ranks for the preconditioner explicit.

Acknowledgements. R.B. and M.S acknowledge support by the Dutch Research Council (NWO) via grant OCENW.KLEIN.183.

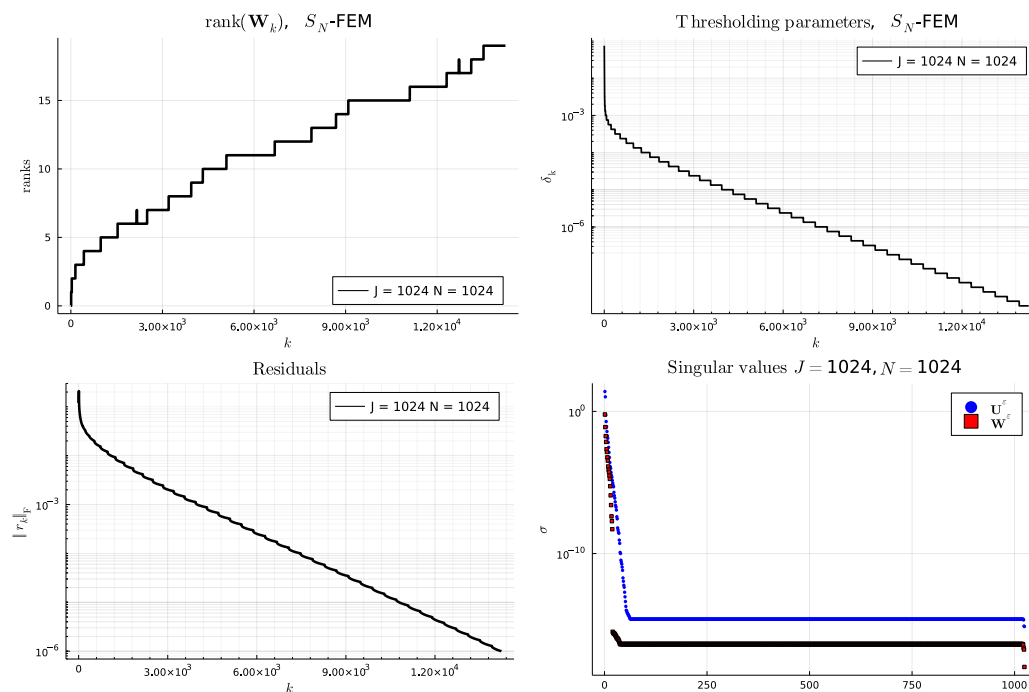


FIGURE 5.4. Behaviour of iterates ranks (top left), thresholding parameter (top right), Frobenius norm of the residuals (bottom left) and singular values of both \mathbf{W}^ϵ and \mathbf{U}^ϵ (bottom right), for the S_N -FEM method applied to test case (5.4).

REFERENCES

- [1] V. AGOSHKOV, *Boundary value problems for transport equations*, Model. Simul. Sci. Eng. Technol., Birkhäuser Boston, Inc., Boston, MA, 1998, <https://doi.org/10.1007/978-1-4612-1994-1>.
- [2] B. AHMEDOV, M. A. GREPL, AND M. HERTY, *Certified reduced-order methods for optimal treatment planning*, Math. Models Methods Appl. Sci., 26 (2016), pp. 699–727, <https://doi.org/10.1142/S0218202516500159>.
- [3] G. ALEXANDRAKIS, F. R. RANNOU, AND C. F. ARION, *Tomographic bioluminescence imaging by use of a combined optical-pet (opet) system: a computer simulation feasibility study*, Phys. Med. Biol., 51 (2005), pp. 391–409, <https://doi.org/10.1080/10407790600964583>.
- [4] S. R. ARRIDGE AND J. C. SCHOTLAND, *Optical tomography: forward and inverse problems*, Inverse Problems, 25 (2009), pp. 123010, 59, <https://doi.org/10.1088/0266-5611/25/12/123010>.
- [5] M. BACHMAYR, *Low-rank tensor methods for partial differential equations*, Acta Numer., 32 (2023), pp. 1–121, <https://doi.org/10.1017/S0962492922000125>.
- [6] M. BACHMAYR AND W. DAHMEN, *Adaptive low-rank methods: problems on Sobolev spaces*, SIAM J. Numer. Anal., 54 (2016), pp. 744–796, <https://doi.org/10.1137/140978223>.
- [7] M. BACHMAYR AND R. SCHNEIDER, *Iterative methods based on soft thresholding of hierarchical tensors*, Found. Comput. Math., 17 (2017), pp. 1037–1083, <https://doi.org/10.1007/s10208-016-9314-z>.
- [8] R. BARDIN, F. BERTRAND, O. PALII, AND M. SCHLOTTBOM, *A phase-space discontinuous galerkin approximation for the radiative transfer equation in slab geometry*, Computational Methods in Applied Mathematics, (2024), <https://doi.org/10.1515/cmam-2023-0090>.
- [9] G. BEYLKIN AND L. MONZÓN, *Approximation by exponential sums revisited*, Appl. Comput. Harmon. Anal., 28 (2010), pp. 131–149, <https://doi.org/10.1016/j.acha.2009.08.011>.
- [10] K. M. CASE AND P. F. ZWEIFEL, *Linear transport theory*, Addison-Wesley Publishing Co., Reading, Mass.-London-Don Mills, Ont., 1967.
- [11] S. CHANDRASEKHAR, *Radiative transfer*, Dover Publications, Inc., New York, 1960.
- [12] W. DAHMEN, F. GRUBER, AND O. MULA, *An adaptive nested source term iteration for radiative transfer*

- equations, *Math. Comp.*, 89 (2020), pp. 1605–1646, <https://doi.org/10.1090/mcom/3505>.
- [13] R. A. DEVORE, *Nonlinear approximation*, *Acta Numer.*, 7 (1998), pp. 51–150, <https://doi.org/10.1017/S0962492900002816>.
- [14] J. DÖLZ, H. EGGER, AND M. SCHLOTTBOM, *A model reduction approach for inverse problems with operator valued data*, *Numerische Mathematik*, 148 (2021), pp. 889–917, <https://doi.org/10.1007/s00211-021-01224-5>, <http://dx.doi.org/10.1007/s00211-021-01224-5>.
- [15] J. J. DUDERSTADT AND W. R. MARTIN, *Transport theory*, A Wiley-Interscience Publication, John Wiley & Sons, New York-Chichester-Brisbane, 1979.
- [16] H. EGGER AND M. SCHLOTTBOM, *A mixed variational framework for the radiative transfer equation*, *Math. Models Methods Appl. Sci.*, 22 (2012), pp. 1150014, 30, <https://doi.org/10.1142/S021820251150014X>.
- [17] H. EGGER AND M. SCHLOTTBOM, *A perfectly matched layer approach for P_N -approximations in radiative transfer*, *SIAM J. Numer. Anal.*, 57 (2019), pp. 2166–2188, <https://doi.org/10.1137/18M1172521>, <https://doi.org/10.1137/18M1172521>.
- [18] K. F. EVANS, *The spherical harmonics discrete ordinate method for three-dimensional atmospheric radiative transfer*, *J. Atmospheric Sci.*, 55 (1998), pp. 429–446, [https://doi.org/10.1175/1520-0469\(1998\)055<0429:TSHDOM>2.0.CO;2](https://doi.org/10.1175/1520-0469(1998)055<0429:TSHDOM>2.0.CO;2).
- [19] W. GAUTSCHI AND C. GIORDANO, *Luigi Gatteschi's work on asymptotics of special functions and their zeros*, *Numer. Algorithms*, 49 (2008), pp. 11–31, <https://doi.org/10.1007/s11075-008-9208-5>.
- [20] K. GRELLA AND C. SCHWAB, *Sparse discrete ordinates method in radiative transfer*, *Comput. Methods Appl. Math.*, 11 (2011), pp. 305–326, <https://doi.org/10.2478/cmam-2011-0017>.
- [21] K. GRELLA AND C. SCHWAB, *Sparse tensor spherical harmonics approximation in radiative transfer*, *J. Comput. Phys.*, 230 (2011), pp. 8452–8473, <https://doi.org/10.1016/j.jcp.2011.07.028>.
- [22] J. KÓPHÁZI AND D. LATHOUWERS, *A space-angle DGFEM approach for the Boltzmann radiation transport equation with local angular refinement*, *J. Comput. Phys.*, 297 (2015), pp. 637–668, <https://doi.org/10.1016/j.jcp.2015.05.031>.
- [23] J. KUSCH AND P. STAMMER, *A robust collision source method for rank adaptive dynamical low-rank approximation in radiation therapy*, *ESAIM Math. Model. Numer. Anal.*, 57 (2023), pp. 865–891, <https://doi.org/10.1051/m2an/2022090>.
- [24] S. LARRSON AND V. THOMÉE, *Partial Differential Equations with Numerical Methods*, Texts in Applied Mathematics, Springer Berlin, 2003.
- [25] E. W. LARSEN, *The nature of transport calculations used in radiation oncology*, *Transport Theor. Stat.*, 26 (1997), pp. 739–763, <https://doi.org/10.1080/00411459708224421>.
- [26] X. MENG, S. WANG, G. TANG, J. LI, AND C. SUN, *Stochastic parameter estimation of heterogeneity from crosswell seismic data based on the mont carlo radiative transfer theory*, *J. Geophys. Eng.*, 14 (2017), pp. 621–633, <https://doi.org/10.1088/1742-2140/aa6130>.
- [27] O. PALII AND M. SCHLOTTBOM, *On a convergent DSA preconditioned source iteration for a DGFEM method for radiative transfer*, *Comput. Math. Appl.*, 79 (2020), pp. 3366–3377, <https://doi.org/10.1016/j.camwa.2020.02.002>.
- [28] Z. PENG, R. G. McCLARREN, AND M. FRANK, *A low-rank method for two-dimensional time-dependent radiation transport calculations*, *J. Comput. Phys.*, 421 (2020), pp. 109735, 18, <https://doi.org/10.1016/j.jcp.2020.109735>.
- [29] M. RUSTAMZHON, D. PRESS, G. K. BASKARAN, S. SADEGHI, AND S. NIZAMOGLU, *Unravelling radiative energy transfer in solid-state lighting*, *J. Appl. Phys.*, 123 (2018), <https://doi.org/10.1063/1.5008922>.
- [30] S. SCHOLZ AND H. YSERENTANT, *On the approximation of electronic wavefunctions by anisotropic Gauss and Gauss-Hermite functions*, *Numer. Math.*, 136 (2017), pp. 841–874, <https://doi.org/10.1007/s00211-016-0856-4>.
- [31] K. STAMNES, G. THOMAS, AND J. STAMNES, *Radiative transfer in the atmosphere and ocean*, Modeling and Simulation in Science, Engineering and Technology, Cambridge University Press, 2nd ed., 2017, <https://doi.org/10.1017/9781316148549>.
- [32] F. G. TRICOMI, *Sugli zeri dei polinomi sferici ed ultrasferici*, *Ann. Mat. Pura Appl. (4)*, 31 (1950), pp. 93–97, <https://doi.org/10.1007/BF02428258>.
- [33] G. WIDMER, R. HIPTMAIR, AND C. SCHWAB, *Sparse adaptive finite elements for radiative transfer*, *J. Comput. Phys.*, 227 (2008), pp. 6071–6105, <https://doi.org/10.1016/j.jcp.2008.02.025>.
- [34] H. YSERENTANT, *On the expansion of solutions of Laplace-like equations into traces of separable higher dimensional functions*, *Numer. Math.*, 146 (2020), pp. 219–238, <https://doi.org/10.1007/s00211-020-01138-8>.
- [35] J. M. ZHAO AND L. H. LIU, *Second-order radiative transfer equation and its properties of numerical solution using the finite-element method*, *Numer. Heat Transf. B*, 51 (2007), pp. 391–409, <https://doi.org/10.1080/10407790600964583>.